

The spin- $\frac{1}{2}$ J_1 - J_2 model on the body-centered cubic lattice

R. Schmidt,* J. Schulenburg, and J. Richter

Institut für Theoretische Physik, Universität Magdeburg, P.O.Box 4120, D-39016 Magdeburg, Germany

D. D. Betts

Department of Physics, Dalhousie University, Halifax, N.S., Canada, B3H 3J5

(Dated: May 21, 2019)

Using exact diagonalization (ED) and linear spin wave theory (LSWT) we study the influence of frustration and quantum fluctuations on the magnetic ordering in the ground state of the spin- $\frac{1}{2}$ J_1 - J_2 Heisenberg antiferromagnet (J_1 - J_2 model) on the body-centered cubic (bcc) lattice. Contrary to the J_1 - J_2 model on the square lattice, we find for the bcc lattice that frustration and quantum fluctuations do not lead to a quantum disordered phase for strong frustration. The results of both approaches (ED, LSWT) suggest a first order transition at $J_2/J_1 \approx 0.7$ from the two-sublattice Néel phase at low J_2 to a collinear phase at large J_2 .

PACS numbers: Valid PACS appear here

I. INTRODUCTION

The properties of the two-dimensional (2d) J_1 - J_2 model have attracted a great deal of interest during the last decade (see e.g. Refs. [1, 2, 3, 4, 5, 6, 7, 8, 9, 10, 11] and references therein). Now it seems to be well-accepted that for the square lattice there is a quantum spin-liquid phase between $J_2/J_1 \approx 0.38$ and $J_2/J_1 \approx 0.60$. The corresponding quantum phase transitions from the Néel ordered state to the spin-liquid state at $J_2/J_1 \approx 0.38$ is of second order, the transition from the spin-liquid state to the collinear state at $J_2/J_1 \approx 0.60$ is of first order. The properties of the spin-liquid phase are a current field of active research. Even additional quantum phase transitions at $(J_2/J_1) \approx 0.34$ and $(J_2/J_1) \approx 0.50$ are discussed [10].

The properties of quantum spin systems strongly depend on the dimensionality. So, contrary to the 2d model, the one-dimensional $J_1 - J_2$ model does not have a Néel ordered ground state, but exhibits a transition from a critical state to a dimer phase at $J_2/J_1 = 0.241$ (see e.g. [12, 13]). Though the tendency to order is more pronounced in three-dimensional (3d) quantum spin systems than in low-dimensional ones a spin-liquid phase is also observed for frustrated 3d systems like the Heisenberg antiferromagnet on the pyrochlore lattice [14, 15].

In this paper we consider the 3d version of the $J_1 - J_2$ model. To cover the possibility to have both Néel phases present in the 2d model we need a bi-bipartite lattice, i.e. a lattice consisting of two interpenetrating bipartite sublattices. The bcc lattice consists of two interpenetrating, identical simple cubic sublattices. Each simple cubic sublattice consists of two interpenetrating, identical fcc lattices. Therefore the bcc lattice is a 3d bi-bipartite cubic lattice.

In what follows we use the exact diagonalization

scheme and the linear spin wave theory to calculate the ground-state properties of the $J_1 - J_2$ model on the bcc lattice and compare the results with the corresponding ones for the square lattice. We will present the ground-state energy, the violation of the Marshall-Peierls sign rule, the sublattice magnetizations and the spin gap of finite lattices in section III. Properties of the infinite lattices will be given in section IV, where the results of the extrapolation of the ground-state energy, the sublattice magnetizations (from ED data) and the corresponding results of the LSWT are shown.

II. THE MODEL

The Hamiltonian of the J_1 - J_2 model is

$$H = J_1 \sum_{\langle i,j \rangle} \mathbf{S}_i \mathbf{S}_j + J_2 \sum_{[i,j]} \mathbf{S}_i \mathbf{S}_j, \quad (1)$$

where $J_1 = 1$ is the nearest-neighbor, and $J_2 \geq 0$ is the frustrating next-nearest-neighbor Heisenberg exchange. We are interested in the extreme quantum case, i.e. we consider the spin quantum number is $s = 1/2$.

The classical ground state for the bcc lattice corresponds to that of the square lattice: For $J_2/J_1 < \alpha_c$ it is a usual two-sublattice Néel state whereas for $J_2/J_1 > \alpha_c$ an antiferromagnet with four sublattices is realized. The first-order transition point α_c depends on the coordination numbers $\alpha_c = z_1/(2z_2)$, where z_1 is the number of nearest-neighbors (J_1 bonds) and z_2 of next-nearest-neighbors (J_2 bonds). Consequently we have $\alpha_c = 1/2$ for the square lattice but $\alpha_c = 2/3$ for the bcc lattice. Therefore we define as the appropriate parameter of frustration

$$p = \frac{J_2 z_2}{J_1 z_1} \quad (2)$$

and we have $p_c^{square} = p_c^{bcc} = 1/2$.

*Electronic address: reimar.schmidt@physik.uni-magdeburg.de

TABLE I: The ten finite bcc lattices are used for exact diagonalization. $\mathbf{l}_1, \mathbf{l}_2, \mathbf{l}_3$ are the three edge vectors in upper triangle lattice form. N is the Number of sites and $\alpha = A, B, C, D, \dots$, is an additional label corresponding to a notation used in [17] to distinguish finite lattices with identical N .

$N\alpha$	edge vectors		
	\mathbf{l}_1	\mathbf{l}_2	\mathbf{l}_3
24C	(2,0,10)	(0,2, 6)	(0,0,24)
28D	(2,0,10)	(0,2, 6)	(0,0,28)
32D	(2,2, 4)	(0,8, 0)	(0,0, 8)
32F	(2,0, 6)	(0,4, 8)	(0,0,16)
32H	(2,0,10)	(0,2, 6)	(0,0,32)
32J	(4,0, 4)	(0,4, 4)	(0,0, 8)
32K	(2,0, 6)	(0,4, 4)	(0,0,16)
36A	(2,0,10)	(0,2, 6)	(0,0,36)
36B	(2,0,14)	(0,2,10)	(0,0,36)
36C	(2,2, 4)	(0,6, 6)	(0,0,12)

III. EXACT DIAGONALIZATION

A. The generation of finite bcc lattices

The generation of finite 3d lattices with periodic boundary conditions is less transparent than for 2d lattices. As has been recently pointed out by Betts and coworkers [16, 17, 18] the use of a triple of edge vectors in upper triangular lattice form (utlf) [19] leads to a systematic generation of finite 3d lattices. In this paper we use the utlf edge vectors and follow strictly Refs. [17, 18]. There are altogether 10 finite bcc lattices with $N \leq 36$ listed in Table I, which fulfill the following three conditions: (i) Every site i of the bcc lattices should have 8 nearest and 6 next-nearest neighbors, which means that they have the full number of nearest and next-nearest neighbors. (ii) The finite lattices should be bi-bipartite in order to avoid frustration due to boundary conditions for $p = 0$ and $p \rightarrow \infty$. (Notice, that finite bcc lattices may be not bi-bipartite even though the infinite bcc lattice is.) (iii) Furthermore they should be topologically distinct, i.e. the spin Hamiltonian (1) should exhibit different physical properties.

B. Ground-state energy

The ground-state energy gives first insight in the nature of possible zero-temperature phase transitions. A kink in $E_0(p)$ (respectively a jump in the first derivative dE_0/dp) signals a first order transition, whereas a smooth dE_0/dp is compatible with second order transitions. Furthermore the maximum in $E_0(p)$ indicates the point of maximal frustration. The ground-state energy for the classical model consists of two straight lines $E_0^{clas}(p) = (p-1)N$ for $p \leq 0.5$ and $E_0^{clas}(p) = -pN$ for $p \geq 0.5$ with a kink (maximum) at $p = 0.5$.

The quantum ground state $|\Psi_0\rangle$ is a singlet eigen state

TABLE II: The ground-state energy per site of the 10 considered finite bcc lattices for different values of J_2 ($J_1 = 1$).

$N\alpha$	E_0/N		
	$J_2 = 0$	$J_2 = 0.7$	$J_2 = 1.3333$
24C	-1.21305	-0.73883	-1.34537
28D	-1.20223	-0.73003	-1.32544
32D	-1.19572	-0.72851	-1.31225
32F	-1.19512	-0.72744	-1.31217
32H	-1.19474	-0.72708	-1.31189
32J	-1.19440	-0.74003	-1.31688
32K	-1.19408	-0.73203	-1.31423
36A	-1.18953	-0.72119	-1.30021
36B	-1.19264	-0.72180	-1.30145
36C	-1.19278	-0.72248	-1.30149

of total spin for all J_2 . In analogy to the square lattice [2] $|\Psi_0\rangle$ of finite bcc lattices with $N \bmod 8 = 0$ has the same symmetry for small and large J_2 , whereas the ground-state symmetry for lattices with $N \bmod 4 = 0$ but $N \bmod 8 \neq 0$ is different for small and large J_2 . The change of symmetry appears near the maximum of frustration.

For the quantum model we show exact-diagonalization results of E_0/N for three different values of frustration in Table II. While $J_2 = 0$ and $J_2 = 1.3333$ correspond to zero or small frustration, $J_2 = 0.7$ is in the region of strong frustration.

For the sake of clearness we present in the figures only results of selected finite lattices. To illustrate the finite-size effects in the most of the subsequent figures we have presented curves for the smallest ($N=24$) and the largest ($N=36$) lattices, where for $N = 36$ we have chosen the lattice 36C having highest symmetry. Note, that the curves for lattices of identical N look very similar.

For comparison with the square lattice we have data up to $N = 6 \times 6 = 36$. However, we decided to compare

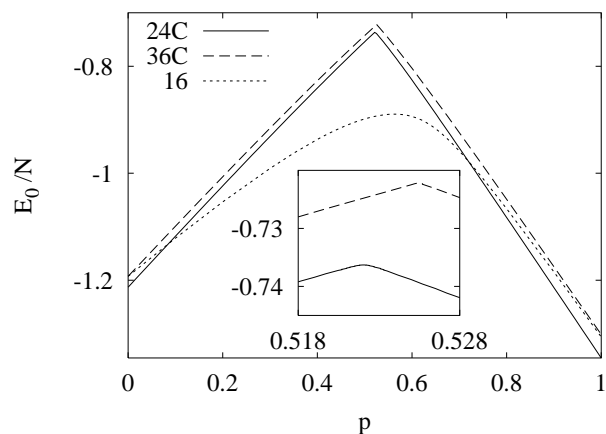


FIG. 1: Ground-state energy per site for the bcc lattices 24C, 36C and for the square lattice with $N = 16$ versus p .

with $N = 4 \times 4 = 16$ (edge vectors $l_1 = (4, 0)$ and $l_2 = (0, 4)$) in order to have comparable characteristic lengths $L_{3d} \propto N^{1/3}$ and $L_{2d} \propto N^{1/2}$. Further, we mention that the square lattice of $N = 16$ contains 5 neighborhood shells, whereas some of the more dense finite bcc lattices with $N = 32$ and $N = 36$ contain even more.

In Fig. 1 one finds the ground-state energies of the bcc lattices 24C, 36C and for comparison the $N = 16$ square lattice. To have comparable curves we shifted the ground-state energy of the square lattice so that it coincides with the ground-state energy of the bcc lattice 36C at $p = 0$. Fig. 1 illustrates that, contrary to the 2d model, the ground-state energy of the 3d bcc lattice behaves very similarly to the classical model.

C. Ground-State Phase Relationships

The phase relationships of the Ising basis states $|n\rangle$ in the ground state $|\Psi_0\rangle$ of the bipartite Heisenberg antiferromagnet (i.e. $J_2 = 0$ in (1)) follow the Marshall-Peierls sign rule [20]. This sign rule can be formulated as

$$|\Psi_0\rangle = \sum_n c_n |n\rangle, \quad c_n > 0. \quad (3)$$

Here the Ising states $|n\rangle$ are defined by

$$|n\rangle \equiv (-1)^{N/2 - M_A} |m_1\rangle \otimes |m_2\rangle \otimes \dots \otimes |m_N\rangle, \quad (4)$$

where $|m_i\rangle$, $i = 1, \dots, N$, are the eigenstates of the site spin operator S_i^z (i.e. $m_i = \pm \frac{1}{2}$), $M_A = \sum_{i \in A} m_i$, where A labels one of the two equivalent sublattices. As pointed out in [4, 5] and very recently in [11] the sign rule may survive some frustration but is clearly violated for the square lattice in the strongly frustrated spin-liquid region. Hence we can use the violation of the sign rule

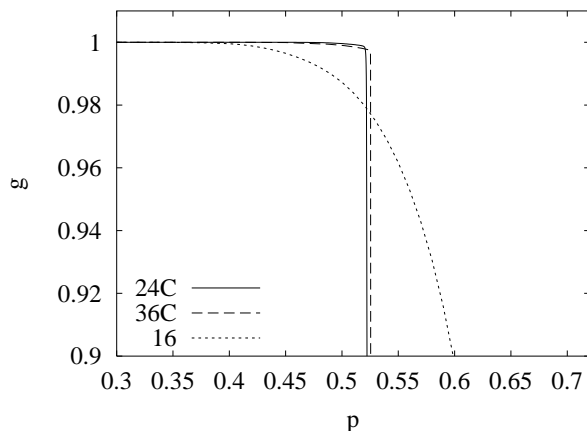


FIG. 2: The weight g of basis states $|n\rangle$ fulfilling the Marshall-Peierls sign rule for the bcc lattice 24C, 36C and the square lattice with $N = 16$ versus p . On the bcc lattices the sign rule is completely fulfilled up to $p = 0.4$ and 99.8% fulfilled at $p = 0.51$.

TABLE III: Sublattice magnetizations m^2 and m_α^2 of the 10 considered bcc lattices for different values of J_2 .

N α	m^2	m_α^2
	$J_2 = 0$	$J_2 = 1.3333$
24C	0.09362	0.11006
28D	0.09057	0.10429
32D	0.08787	0.09958
32F	0.08800	0.09959
32H	0.08811	0.09964
32J	0.08819	0.09897
32K	0.08827	0.09933
36A	0.08600	0.09605
36B	0.08516	0.09562
36C	0.08509	0.09561

as an indication of the breakdown of the two-sublattice Néel state. In Fig. 2 one finds the weight $g = \sum_n (c_n)^2$ of the Ising states $|n\rangle$ fulfilling the Marshall-Peierls sign rule (i.e. the sum \sum_n is restricted to the subset of states having $c_n > 0$) for two finite bcc lattices and the $N = 16$ square lattice. For the $J_1 - J_2$ model on the bcc lattice the rule is violated almost discontinuously at that point where the ground-state energy has its maximum. This is a hint to a very drastic change of the ground state on the bcc lattice around $p = 0.525$ which can be attributed to an abrupt breakdown of the two-sublattice Néel state. On the other hand for the $J_1 - J_2$ model on the square lattice the violation of the sign rule starts smoothly and becomes significant near $p = 0.4$ where the second-order transition to the spin-liquid state takes place.

D. Sublattice magnetizations

Of course the most important parameter to study Néel ordering is the sublattice magnetization. In finite systems the conventional antiferromagnetic LRO, that is re-

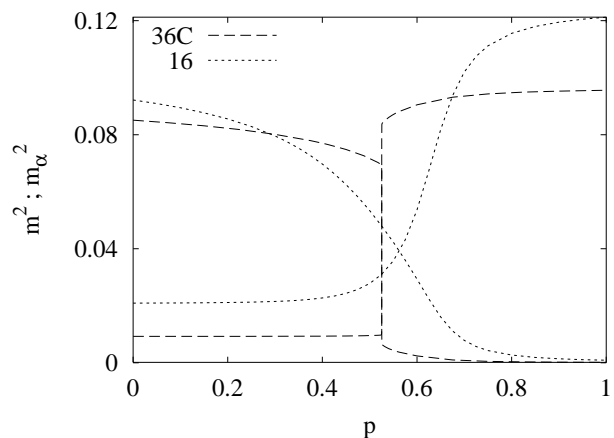


FIG. 3: Sublattice magnetizations m^2 and m_α^2 of the bcc lattice 36C and the square lattice ($N=16$) vs. p .

alized for small p , has to be described by the square of the sublattice magnetization of one spin component

$$m^2 = \langle [\frac{1}{N} \sum_{i=1}^N \tau_i S_i^z]^2 \rangle, \quad \tau_{i \in A} = 1, \quad \tau_{i \in B} = -1. \quad (5)$$

For large values of p the order parameter

$$m_\alpha^2 = \langle [\frac{1}{N/2} \sum_{i_\alpha=1}^{N/2} \tau_{i,\alpha} S_{i_\alpha}^z]^2 \rangle, \quad \tau_{i,\alpha} = \pm 1, \quad \alpha = A, B \quad (6)$$

is relevant. m_α^2 describes the antiferromagnetic order within the initial sublattices A and B . $\tau_{i,\alpha}$ is the corresponding staggered factor. In Table III we give the sublattice magnetizations of the ten finite bcc lattices for $J_2 = 0$ and $J_2 = 1.3333$. The behavior of the order parameters m^2 and m_α^2 shown in Fig. 3 again illustrates, that the influence of the frustration on the ground-state properties is basically different for the square and bcc lattice and suggests a direct first-order transition between both Néel phases for the bcc lattice. A more detailed presentation of the transition region is given in Fig. 4. One finds that the position of the transition only slightly depends on size and symmetry of the finite lattices. Moreover, the width of transition region is getting smaller with growing N . Again we mention that the region of transition is related to the maximum of E_0 and the significant violation of the Marshall-Peierls sign rule.

E. Spin gap

Another indication for a possible quantum disordered spin-liquid state is the spin gap, i.e. the gap Δ_{ST} between the singlet ground state and the first triplet excitation. In Néel ordered systems we have Goldstone modes and no

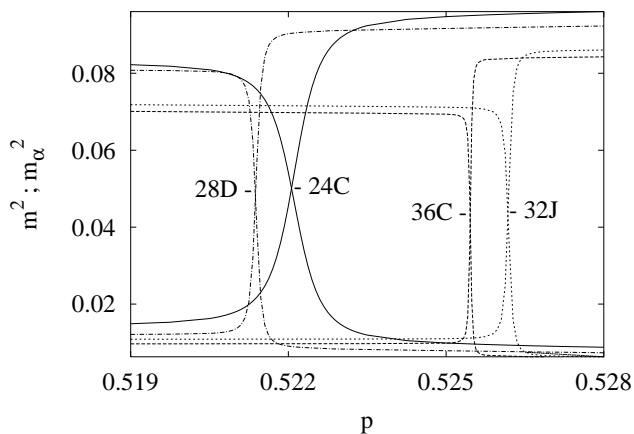


FIG. 4: Sublattice magnetizations m^2 and m_α^2 of the bcc lattice 36C, 32D, 28D and 24C near the phase transition point $p \approx 0.52$.

spin gap is observed in the thermodynamic limit. Contrary to this, quantum disorder is accompanied by the opening of a spin gap. The corresponding results shown in Fig. 5 support our previous discussion that there is no hint on quantum disorder for the spin- $\frac{1}{2}$ J_1 - J_2 model on the bcc lattice.

IV. INFINITE BCC LATTICES

A. Finite-Size Extrapolation

To obtain properties of the infinite bcc lattice we extrapolate the ED data of all ten lattices listed in Table I. The finite-size extrapolation is a well elaborated approximation scheme successfully applied to many 2d quantum spin systems like the $J_1 - J_2$ model on the square lattice [2]. But even for 3d lattices this scheme may lead to precise data for the infinite lattice [16, 17, 18]. The corresponding scaling laws are known from literature [21, 22, 23]. The scaling equation for ground-state energy per site $\epsilon = E_0/N$ of the bcc lattice is

$$\epsilon(L) = \epsilon(\infty) + A_4 L^{-4} + \dots \quad (7)$$

and for the sublattice magnetization

$$m^2(L) = m^2(\infty) + B_2 L^{-2} + \dots \quad (8)$$

with $L = N^{1/3}$.

The same relation is valid for m_α^2 . The results are presented in Figs. 6 and 7. The discussion of the data is given below.

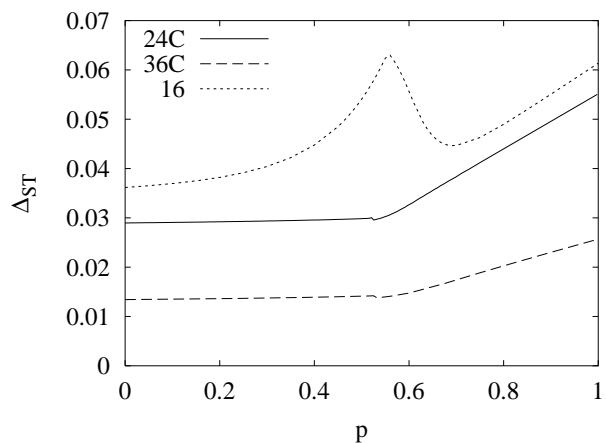


FIG. 5: Spin gap Δ_{ST} , i.e. the gap to the first triplet excitation for the bcc lattices 24C, 36C and the square lattice with $N = 16$ vs. p .

B. Linear spin wave theory (LSWT)

1. LSWT for small J_2

Starting from the classical two-sublattice Néel state we choose a two-boson representation of the Hamiltonian (1). Rewriting the spin operators of the Hamiltonian in terms of bose operators by using the usual Holstein-Primakoff transformation and taking into account only quadratic terms in the bose operators, we obtain a bosonic Hamiltonian in Fourier transformed representation

$$H = s^2 N(-8 + 6p) + \sum_{\mathbf{k}} \{A_{\mathbf{k}}(a_{\mathbf{k}}^{\dagger} a_{\mathbf{k}} + b_{\mathbf{k}}^{\dagger} b_{\mathbf{k}}) + B_{\mathbf{k}}(a_{\mathbf{k}} b_{-\mathbf{k}} + a_{\mathbf{k}}^{\dagger} b_{-\mathbf{k}}^{\dagger})\} \quad (9)$$

with the coefficients

$$A_{\mathbf{k}} = s(8 - 6p(1 - \gamma_{2\mathbf{k}})) \quad (10)$$

$$B_{\mathbf{k}} = 8s\gamma_{1\mathbf{k}}. \quad (11)$$

The structure factors of nearest neighbors and next-nearest neighbors are given by

$$\gamma_{1\mathbf{k}} = \cos k_x \cos k_y \cos k_z \quad (12)$$

$$\gamma_{2\mathbf{k}} = \frac{1}{3}(\cos 2k_x + \cos 2k_y + \cos 2k_z). \quad (13)$$

The ground-state energy per site is then

$$E_0/N = s^2(-8 + 6p) + \frac{1}{N} \sum_{\mathbf{k}} (\omega_{\mathbf{k}} - A_{\mathbf{k}}) \quad (14)$$

with $\omega_{\mathbf{k}} = \sqrt{A_{\mathbf{k}}^2 - B_{\mathbf{k}}^2}$. The sublattice magnetization $m = \langle S_i^z \rangle$ is

$$m = s - \frac{1}{N} \sum_{\mathbf{k}} \left(-\frac{1}{2} + \frac{A_{\mathbf{k}}}{2\omega_{\mathbf{k}}} \right). \quad (15)$$

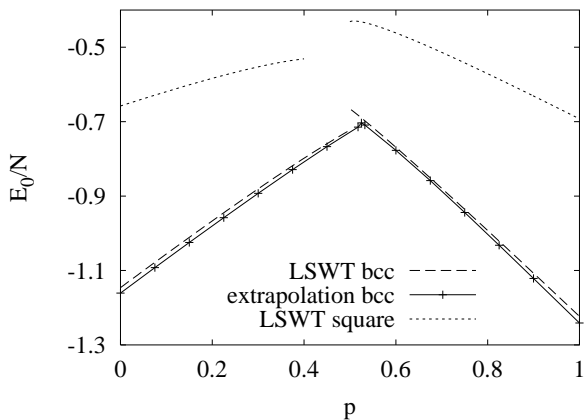


FIG. 6: LSWT data for the ground-state energies E_0 of the infinite bcc lattice (dashed line) and square lattice (dotted line) as well as the extrapolated ED data for E_0 (solid line with data points) vs. p .

2. LSWT for large J_2

The classical ground state of the $J_1 - J_2$ model on the bcc lattice for large J_2 consists of two interpenetrating Néel states each living on the initial sublattices A and B . The two Néel states are energetically decoupled, i.e. the angle θ between the staggered magnetization on A and B is arbitrary for classical spins. For the quantum model we start with arbitrary θ and use as quantization axis the local orientation of the spins in the classical ground state. The further procedure is the same as for small J_2 but the bosonic Hamiltonian now contains the angle θ . By means of the Hellmann-Feynman theorem [24] $\langle \partial H(\theta) / \partial \theta \rangle = \partial E(\theta) / \partial \theta$ it can be easily found that in the quantum model the collinear state ($\theta = 0$ or π) has lowest energy. This lifting of the continuous degeneracy of the classical ground state by quantum fluctuations ('order from disorder effect') is also found for the square lattice [25]. For $\theta = 0$ the bosonic Hamiltonian reads

$$H = -6Nps^2 + \sum_{\mathbf{k}} \left\{ A(a_{\mathbf{k}}^{\dagger} a_{\mathbf{k}} + b_{\mathbf{k}}^{\dagger} b_{\mathbf{k}}) + [C_{\mathbf{k}}(b_{\mathbf{k}} a_{\mathbf{k}}^{\dagger} - b_{\mathbf{k}}^{\dagger} a_{-\mathbf{k}}^{\dagger}) - B_{\mathbf{k}}(a_{\mathbf{k}} a_{-\mathbf{k}} + b_{\mathbf{k}} b_{-\mathbf{k}}) + h.c.] \right\} \quad (16)$$

where

$$A = 6sp \quad (17)$$

$$B_{\mathbf{k}} = 3sp\gamma_{2\mathbf{k}} \quad (18)$$

$$C_{\mathbf{k}} = 4s(\cos k_x \cos k_y \cos k_z + i \sin k_x \sin k_y \sin k_z). \quad (19)$$

Then the ground-state energy per site is

$$E_0/N = -6s^2p + \frac{1}{N} \sum_{\mathbf{k}} \left(\frac{\omega_{1\mathbf{k}}}{2} + \frac{\omega_{2\mathbf{k}}}{2} - A \right) \quad (20)$$

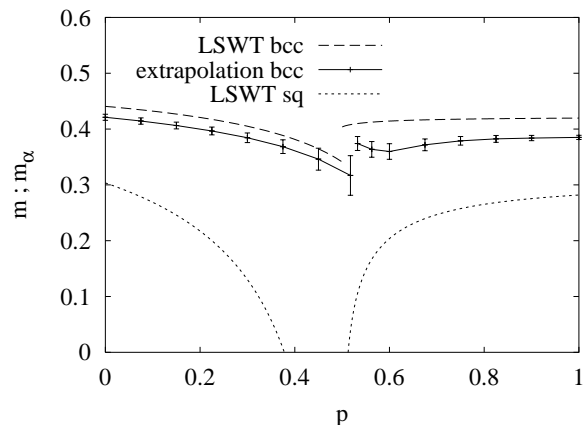


FIG. 7: LSWT data for the sublattice magnetizations m of the infinite bcc lattice (dashed line) and square lattice (dotted line) as well as extrapolated ED data for $\sqrt{3m^2(\infty)}$ and $\sqrt{3m_{\alpha}^2(\infty)}$ (solid line with data points) vs. p . The error bars indicate the standard deviation of the finite-size extrapolation.

with the modes

$$\omega_{1\mathbf{k}} = \sqrt{A^2 - 4B_{\mathbf{k}}^2 + F_{\mathbf{k}}}; \quad \omega_{2\mathbf{k}} = \sqrt{A^2 - 4B_{\mathbf{k}}^2 - F_{\mathbf{k}}} \quad (21)$$

and the function

$$F_{\mathbf{k}} = \left\{ (C_{\mathbf{k}}^2 - C_{\mathbf{k}}^{*2})^2 - 8AB_{\mathbf{k}}(C_{\mathbf{k}}^2 + C_{\mathbf{k}}^{*2}) + 4C_{\mathbf{k}}C_{\mathbf{k}}^*(A^2 + 4B_{\mathbf{k}}^2) \right\}^{1/2}. \quad (22)$$

The sublattice magnetization is written as

$$m_{\alpha} = s - \frac{1}{N} \sum_{\mathbf{k}} \frac{D(\mathbf{k}, \omega_{1\mathbf{k}})}{2\omega_{1\mathbf{k}}(\omega_{1\mathbf{k}}^2 - \omega_{2\mathbf{k}}^2)} - \frac{1}{N} \sum_{\mathbf{k}} \frac{D(\mathbf{k}, \omega_{2\mathbf{k}})}{2\omega_{2\mathbf{k}}(\omega_{2\mathbf{k}}^2 - \omega_{1\mathbf{k}}^2)} \quad (23)$$

with

$$D(\mathbf{k}, \omega_{\mathbf{k}}) = -\omega_{\mathbf{k}}^3 + A\omega_{\mathbf{k}}^2 - (4B_{\mathbf{k}}^2 - A^2)\omega_{\mathbf{k}} + A(4B_{\mathbf{k}}^2 + 2C_{\mathbf{k}}C_{\mathbf{k}}^*) - 2B_{\mathbf{k}}(C_{\mathbf{k}}^2 + C_{\mathbf{k}}^{*2}) - A^3. \quad (24)$$

The results of LSWT and the finite-size extrapolation are shown in Figs.6 and 7. For the limits $J_2 = 0$ and $J_1 = 0$ our LSWT results are in agreement with data for the bcc and the sc lattice given in [23]. Both methods yield similar results. For the ground-state energy we have a good quantitative agreement. Being in the size of the data points, the standard deviation of extrapolated ground-state energy is not shown. For the order parameter the finite-size effects are stronger and the agreement is only qualitative. Both methods suggest a first-order transition for the spin- $\frac{1}{2}$ J_1 - J_2 model on the bcc lattice. The transition point obtained from the ED data is $J_2 \approx 0.7J_1$ (i.e. $p \approx 0.52$) while the LSWT becomes unstable at the classical transition point.

V. CONCLUSION

We have presented spin-wave and exact diagonalization results for the spin- $\frac{1}{2}$ J_1 - J_2 model on the bcc lattice and compare them with those for the square lattice. In general, we observe that the physics for the 3d quantum model is closer to classical behavior since quantum fluctuations and finite-size corrections become less important for higher coordination number and larger dimension.

We are not sure whether the increase of the magnetization m_{α} approaching the transition point from the right (shown in Fig.7) is a real effect. A possible physical origin for an increase may be a stronger coupling of the Néel ordered subsystems A and B due to larger quantum fluctuations or finite-size effects that become more important in the region of strong frustration. From the data for the ground-state energy, the Marshall-Peierls sign rule, the sublattice magnetizations and the spin gap we conclude that the increase from dimension $d=2$ to $d=3$ changes the physical properties basically. The good agreement with the spin wave results support this conclusion. Contrary to the 2d model, in the 3d model we find no indications for a disordered spin-liquid like magnetic phase. Instead we find one transition of first order whereby the results of the extrapolation show a shift of the classical transition point to $p \approx 0.52$.

Acknowledgements: We acknowledge support from the Deutsche Forschungsgemeinschaft (Project No. Ri 615/7-1). Besides we also want to thank Dirk Schmalfuß for fruitful discussions.

-
- [1] P. Chandra and B. Doucot, *Phys. Rev. B* **38**, 9335 (1988).
[2] H.J. Schulz and T.A.L. Ziman, *Europhys. Lett.* **18**, 355 (1992); H.J. Schulz, T.A.L. Ziman and D. Poilblanc *J. Phys. I* **6**, 675 (1996).
[3] J. Richter, *Phys. Rev. B* **47**, 5794 (1993).
[4] K. Retzlaff, J. Richter and N.B. Ivanov, *Z. Phys. B* **93**, 21, (1993).
[5] J. Richter, N.B. Ivanov and K. Retzlaff, *Europhys. Lett.* **25**, 545 (1994).
[6] R.F. Bishop, D.J.J. Farnell and J.B. Parkinson, *Phys. Rev. B* **58**, 6394 (1998).
[7] R.R.P. Singh, Zheng Weihong, C.J. Hamer and J. Oitmaa, *Phys. Rev. B* **60**, 7278 (1999).
[8] V.N. Kotov and O.P. Sushkov, *Phys. Rev. B* **61**, 11820 (2000).
[9] L. Capriotti and S. Sorella, *Phys. Rev. Lett.* **84**, 3173 (2000).
[10] O.P. Sushkov, J. Oitmaa and Zheng Weihong, *Phys. Rev. B* **63**, 104420 (2001).
[11] L. Capriotti, F. Becca, A. Parola and S. Sorella, *Phys. Rev. Lett.* **87**, 97201 (2001).
[12] K. Okamoto and K. Nomura, *Phys. Lett. A* **169**, 433 (1992).
[13] S. Eggert, *Phys. Rev. B* **54**, R9612 (1996).
[14] B. Canals and C. Lacroix, *Phys. Rev. Lett.* **80**, 2933 (1998).
[15] A. Koga and N. Kawakami, *Phys. Rev. B* **63**, 144432 (2001).
[16] G.E. Stewart, D.D. Betts and J.S. Flynn *J. Phys. Soc. Jap.* **66** 3231 (1997).
[17] D.D. Betts, J. Schulenburg, G.E. Stewart, J. Richter and J.S. Flynn, *J. Phys. A: Math. Gen.* **31**, 7685 (1998).
[18] J. Schulenburg, J.S. Flynn, D.D. Betts and J. Richter, *Eur. Phys. J. B* **21**, 191 (2001).
[19] J.N. Lyness, T. Sorevik and P. Keast *Mathematics of Computation* **56** 243 (1991).
[20] W. Marshall, *Proc. Roy. Soc. A* **232**, 48 (1955).
[21] H. Neuberger and T. Ziman, *Phys. Rev. B* **39**, 2608 (1989).
[22] P. Hasenfratz and F. Niedermayer, *Z. Phys. B* **92**, 91

- (1993).
- [23] J. Oitmaa, C.J. Hamer and Zheng Weihong, *Phys. Rev. B* **50**, 3877 (1994).
- [24] R.P. Feynman, *Phys. Rev.* **50**, 340 (1939).
- [25] K. Kubo and T. Kishi, *J. Phys. Soc. Jap.* **60**, 567 (1990).